

ANALYSIS OF 3D PRINTING APPLICATIONS WITH ABS FILAMENT MATERIAL FOR DESIGNING UNMANNED AIRCRAFT BODYBUILDS

Lazuardi Lazuardi^{1✉}, Muhammad Akhlis Rizza², Sugeng Hadi Susilo³, Maryono Maryono⁴

¹PGRI Wiranegara University Pasuruan, Indonesia

^{2,3} State Polytechnic of Malang, Indonesia

⁴ Army Polytechnic of Malang, Indonesia

*Author Email: Atingthok99@gmail.com, muh.akhlis@polinema.ac.id, sugeng.hadi@polinema.ac.id, maryono250375@gmail.com

Article Information

Manuscript Received 2024-04-05
Manuscript Revised 2024-04-16
Manuscript Accepted 2024-04-18
Manuscript Online 2024-04-18

ABSTRACT

This research applies 3D printing technology using ABS filament material in designing the body of an unmanned aircraft. A quantitative approach to the simulation results is used to highlight the technical superiority of unmanned airframes. The analysis includes aspects such as structural strength. These findings provide deep insight into the potential application of 3D printing technology in the aerospace industry, as well as its application to the design, production costs and performance of unmanned aircraft. The research results show that the use of 3D printing with ABS filament has the potential to produce a strong and light aircraft body. From the research, it was found that the ideal layer thickness parameter of 0.1 to 0.2 mm does not exceed half the size of the nozzle diameter of 0.4 mm to produce fine raster fibers on the aircraft body without a crew. From the research it was found that the ideal speed parameter for printing the aircraft body frame unmanned aircraft with ABS filament material at a speed of 30 mm/s to 50 mm/s to produce a stable raster fiber size on the aircraft body and the percentage parameter of a good fill for printing the body frame of an unmanned aircraft is at a value of 20% up to 40%. The research results found the best printing parameters for printing aircraft frames with the parameter formula of 0.15mm 3D layer height, 20% gyroid infill, with a speed of 30mm/s maximum tensile strength reaching 30.7 MPa. By considering the challenges and opportunities associated with the use of 3D printing technology, this research provides a solid foundation for further development in designing and producing unmanned aircraft bodies efficiently and innovatively.

Keywords: 3D printing, ABS Filament, Unmanned aircraft.

1. INTRODUCTION

Fused Deposition Modeling (FDM) technology is a 3D design printing machine in CAD form to be printed into 3D objects [1]. In the aerospace industry, 3D printers have the potential to be used as a means of creating strong and light unmanned aircraft body frames [2], [3], [4]. FDM is a technology that is classified as "Material Extrusion". On an FDM machine, 3D objects are formed using melted resin and then printed layer by layer until a 3D object is formed [5], [6], [7]. Various types of plastic that can be processed using an FDM machine include acrylonitrile butadiene styrene (ABS) and polycarbonate (PC). The movement and direction of the machine print adjusts to the G-code program that has been created [8].

ABS (acrylonitrile butadiene styrene) plastic material is a very versatile material and has the potential to be developed to make the body frame for unmanned aircraft [9]. ABS is popular because it has good material characteristics. ABS material has an average density value

of 1.07 *grams/cm*³ with a tensile strength of 43 MPa [10] ABS material also has the ability to withstand heat reaching 110°C. ABS material has a melting point temperature of 200 °C [11], [12], [13]. From its characteristics, ABS plastic material makes it possible to use it as raw material for making unmanned aircraft frames [14], [15], [16].

To determine the results of printing an unmanned aircraft body frame from 3D printing with good quality and strength, there are various indicators that must be considered: 1. Strength of the 3D printed result, 2. Success of the printing process, 3. Print time (lead time) [17], [18], [19].

2. RESEARCH SIGNIFICANCE

The Cessna 172 Skyhawk is a four-seat, low-wing light aircraft manufactured by the Cessna Aircraft Company. It is one of the most popular aircraft in the history of general aviation and has been used widely throughout the world for a variety of purposes, including flight training, private

aviation, aerial surveying, and monitoring. The researcher's reference for designing the unmanned aircraft was a Cessna 172 Skyhawk training aircraft with registration number PK-HAD. Field observations were carried out in the hangar of the Malang State Polytechnic, Indonesia. The shape of the Cessna 172 Skyhawk aircraft can be seen in Figure 1.



Figure 1. Malang State Polytechnic Hangar

From the results of observations made on a Cessna 172 Skyhawk aircraft with registration number PK-HAD. In the State Polytechnic of Malang hangar, Indonesia, the dimensions and weight specifications for the Cessna 172 Skyhawk training aircraft were obtained which are presented in table 1.

Tabel 1. Spesifikasi dimensi Cessna 172

Cessna 172 dimensions	
Wingspan	11,0 meters
Length	8,28 meters
Height	2,72 meters
Cessna 172 weight	
Empty Weight	1.691 pounds (767 kg)
Maximum Takeoff Weight	2.450 pounds (1.111 kg)
Maximum Landing Weight	2.450 pounds (1.111 kg)

From the results of observations made on a Cessna 172 Skyhawk aircraft with registration number PK-HAD. In the Malang State Polytechnic hangar, Indonesia, the performance specifications for the Cessna 172 Skyhawk training aircraft were obtained which are presented in table 2.

Table 2. Cessna 172 performance specifications

Cessna 172 performance	
Maximum Speed	124 knots (229 km/jam)
Cruising Speed	122 knots (226 km/jam)
Service Height	14.000 kaki (4.267 meter)
Takeoff Distance	690 kaki (210 meter)
Landing Distance	sekitar 520 kaki (158 meter)
Rate of Increase	730 kaki/menit

From the results of field observations carried out in the Malang State Polytechnic hangar, researchers were able to

create a design plan for an unmanned aircraft as shown in Figure 2.

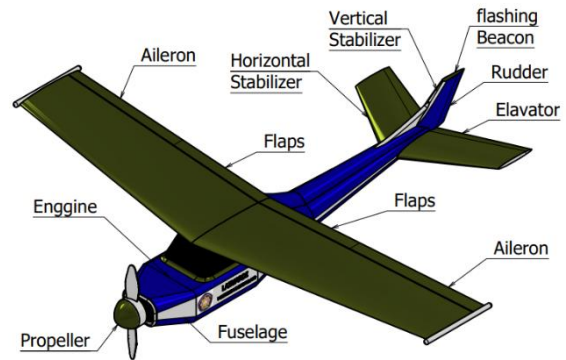


Figure 2. Unmanned aircraft design.

Obtained from the planned design, the aircraft has dimensions and weight specifications shown in table 3.

Table 3. Dimension specifications

Dimensi pesawat tanpa awak	
Wing Span	1009 Milimeters
Length	77,9 Milimeters
Height	121 Milimeters
Empty Weight	6,7 Kilogram.

From table 3 we can explain the view of the aircraft from the perspective of the lateral axis which displays the wing span. It can be seen in Figure 3.

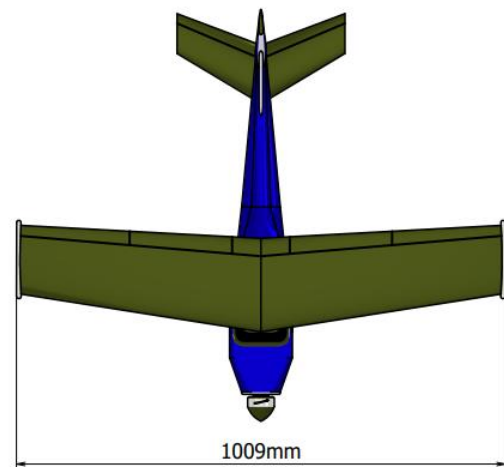


Figure 3. Axis lateral plane view

Table 3 explain the view of the aircraft from the perspective of the longitudinal axis which displays the overall length of the aircraft. It can be seen in Figure 4.

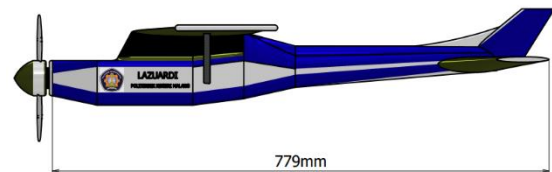


Figure 4. Axis longitudinal view

Table 3 explain the view of the aircraft from the Vertical Axis point of view which displays the overall height of the aircraft. It can be seen in Figure 5.



Figure 5. Axis vertical plane

To engineer strong and light unmanned aircraft frame prints, researchers tried to combine the percentage of infill density with density variations of 20%, 30%, 40% and researchers also combined layer height with variations of 0.1mm, 0.15mm, 0.2mm. By analyzing the combination of infill percentage (the geometric density of the aircraft body fill) and layer height (layer thickness) which are varied. It is hoped that the research will find 3D printing parameters that produce a strong and light aircraft body.

3. RESEARCH METHODS

In the 3D printing process of the aircraft body frame using a 3D printing machine with the Ender 3 Professional brand type, a product from the company Shenzhen Creality 3D Technology, Jin Cheng Yuan, China. Machine specifications can be shown in Table 4 showing the specifications of the Ender 3 Professional machine

Table 4. Ender 3 Professional Specifications.

Parameters	Value
Model Number	Ender 3 Pro
Build Size	220*220*250mm
Machine Size	440*440*465mm
Rated Power	270 watt
Rated Voltage	AC115/230V
Rated Current	4A/2.1A

The filament material used to print the aircraft body frame is the Sunlu brand ABS (acrylonitrile butadiene styrene) polymer, a product of the Zhuhai Sunlu Industrial company, Guangdong, China. Table 5 shows the company's recommended 3D printing temperature standards.

Table 5. ABS Filament Material Specifications.

Rekomendasi Suhu Cetak Filament ABS	
Parameters	Value
Heated bed (°C)	95-110
Extruder Temperature (°C)	220-250

Mechanical test methods and design simulations are used to design unmanned aircraft frame designs. This method is more effective for determining the relationship of several 3D printing parameters to the mechanical strength of the planned aircraft body frame. Figure 6 explains the schematic in this planning:

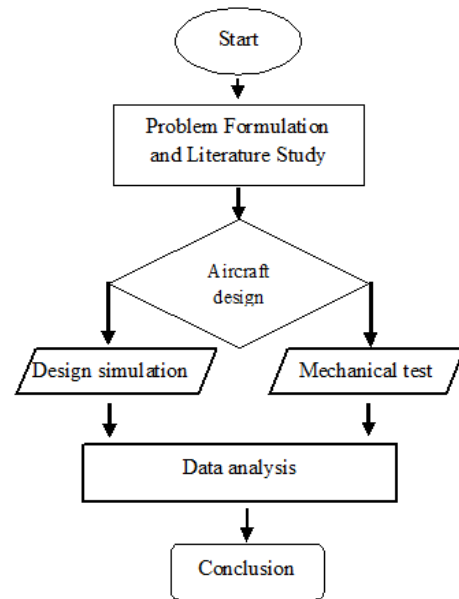


Figure 6. Schematic of the research flow.

Tensile test specimens to determine the mechanical strength of ABS (acrylonitrile butadiene styrene) filament material using the JIS Z2201 standard [20]. Figure 7 explains the standard sizes of JIS Z2201 tensile test specimens.

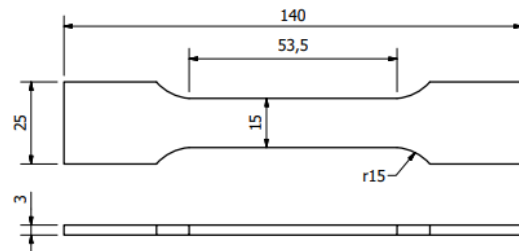


Figure 7. Tensile test specimen dimensions

Table 6 shows the 3D printing parameters which were left constant as controlled variables in this experiment.

Table 6. Controlled Variables.

Parameter	Value
Nozzel diameter (mm)	0,4
Nozzel Temperature (°C)	240
Bed Temperature (°C)	80
Wall Thickness (mm)	1,6

Table 7 shows several 3D printing parameters that were given variations to serve as independent variables in the experiment.

Table 7. Independent Variables Print parameters.

Parameter	Value		
	Low	Middle	High
Speed (mm/s)	30	40	50
Infill density (%)	20	30	40
Layer height (mm)	0,1	0,15	0,2

Mechanical strength testing using the tensile test method on specimens was carried out using the Tarno Grocki Universal Testing Machine. Figure 8 explains the process of the tensile test experiment.



Figure 8. Tensile test process.

4. RESULTS AND DISCUSSION

4.1 Experimental Results

To determine the effect of the combined 3D object printing process parameter formula on the design of the unmanned aircraft frame, the mechanical characteristics were tested using a tensile test, on tensile test specimens using the JIS Z2201 standard, Table 8 explains the results of the tensile test findings as follows:

Table 8. Tensile test results.

Code	Layer height (mm)	Infill density (%)	Speed (mm/s)	Tegangan (MPa)
Ya1	0,1	2	30	26,5
Ya2	0,1	30	40	24
Ya3	0,1	40	50	27,2
Yb1	0,15	20	30	30,7
Yb2	0,15	30	40	30,1
Yb3	0,15	40	50	28,6
Yc1	0,2	20	30	27,7
Yc2	0,2	30	40	28,8
Yc3	0,2	40	50	26,7

From table 8 a performance diagram can be made from the tensile test results which can be seen in figure 9

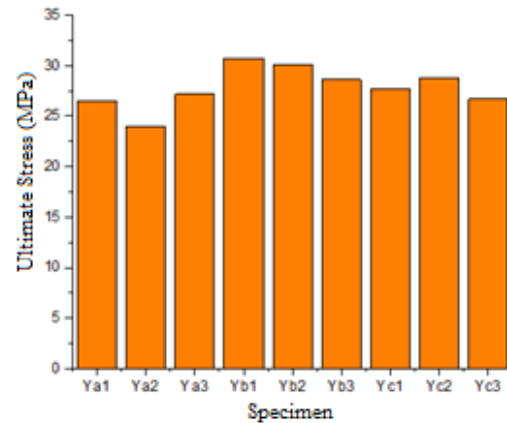


Figure 9. Performance of tensile test results.

From the tensile test results using the JIS Z2201 standard, three 3D object printing parameter formulas were obtained which produced three different qualities. Low quality (Ya2) with a 3D printing parameter formula of layer height 0.1mm, 30% gyroid infill, with a speed of 40mm/s. Maximum tensile stress reaches 24 Mpa. Figure 10 explains the strain and stress graph from the tensile test results of the Low quality print parameter formula.

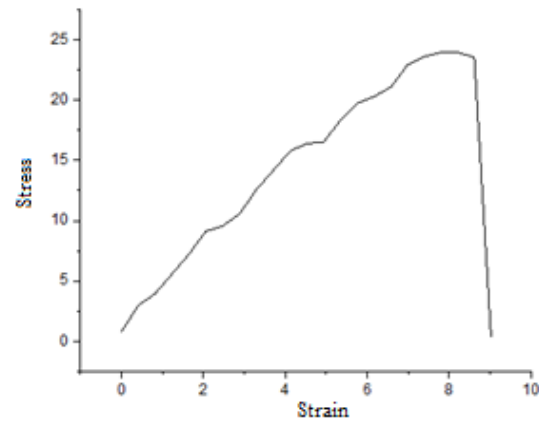


Figure 10. Stress and strain graph for Low Quality print results.

Middel Quality (Yc1) with a 3D layer height formula of 0.2mm, 20% gyroid infill, with a speed of 30mm/s maximum tensile strength reaching 27.7 Mpa. Figure 11 explains the strain and stress graphs from the tensile test results of the Low Middel printing parameter formula.

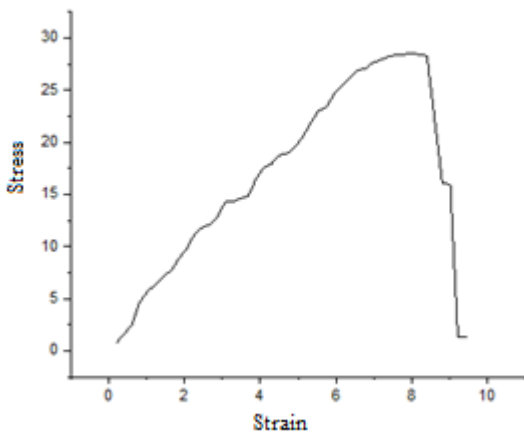


Figure 11. Stress and strain graph for Middle Quality print results.

High Quality (Yb1) with 3D printing parameter formula layer height 0.15mm, gyroid infill 20%, with a speed of 30mm/s maximum tensile strength reaching 30.7 MPa. Figure 12 explains the strain and stress graph of the tensile test results of the High Middel printing parameter formula.

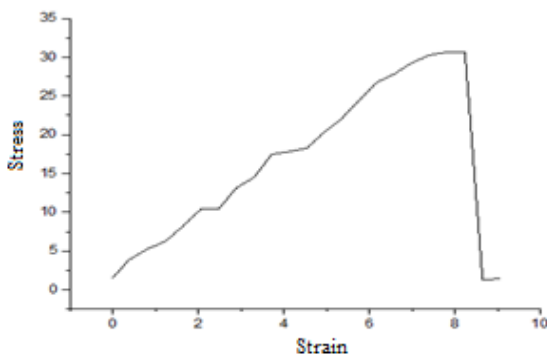


Figure 12. Stress and strain graph for High Quality print results.

4.2 Simulation Results

To determine the strength of the aircraft body, a simulation was carried out on the design of the aircraft body with dimensions as in Figure 2. The simulation was carried out on four parts of the aircraft including: (1) Fuselage, (2) wing, (3) horizontal stabilizer, and (4) vertical stabilizer. To find the maximum stress that occurs on the aircraft when it is in working condition. The simulation carried out loads reaching 100N.

Simulation results of the stress that occurs in the fuselage part which functions as the body of an unmanned aircraft when it receives a load of 100N. It can be seen in Figure 13.

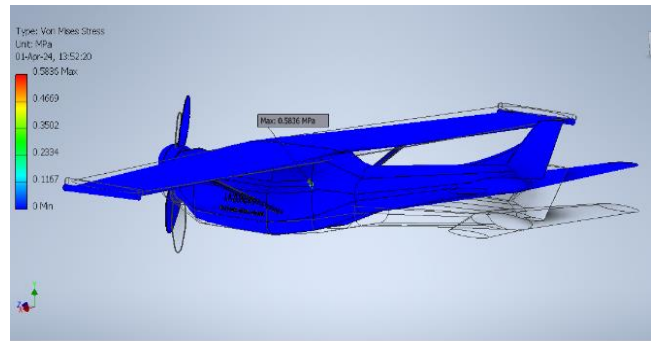


Figure 13. Fuselage stress concentration

If we describe the maximum and minimum stresses that occur in the fuselage section of the aircraft into a graph, they can be seen in Figure 14.



Figure 14. Voltage graph on the fuselage

Figure 14 shows the minimum stress that occurs in the fuselage of the fuselage is 0.161 Mpa, the average stress distribution in the fuselage of the fuselage is 0.350 Mpa, and the maximum stress that occurs in the fuselage of the fuselage is 0.585 Mpa.

Simulation results of the stress that occurs on the wing of an unmanned aircraft when it receives a load of 100N. It can be seen in Figure 15.

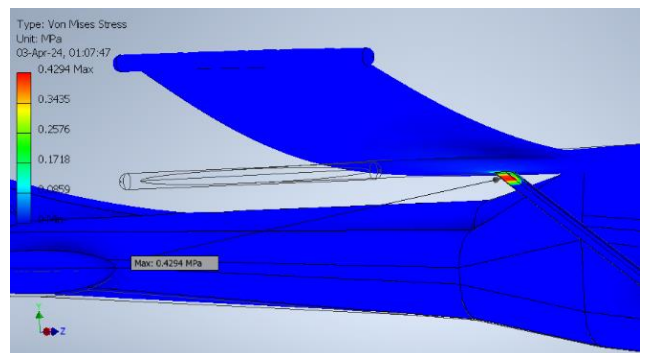


Figure 15. wing stress concentration

If we describe the maximum and minimum stresses that occur on the aircraft wing into a graph, they can be seen in Figure 16.

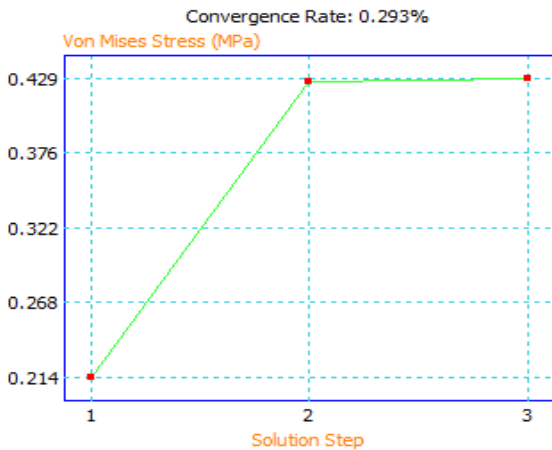


Figure 16. Stress graph on the wing

Figure 16 shows the minimum stress that occurs in the aircraft wing is 0.214 Mpa, the average stress distribution in the aircraft wing is 0.376 Mpa, and the maximum stress that occurs in the aircraft wing is 0.429 Mpa.

Simulation results of the stress that occurs in the horizontal stabilizer section of an unmanned aircraft when it receives a load of 100N. It can be seen in Figure 17 as follows:

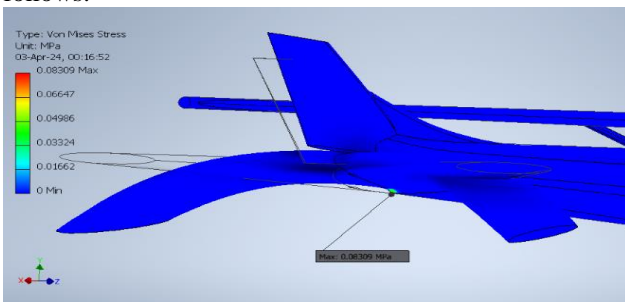


Figure 17. Concentration of horizontal stabilizer.

If we describe the maximum and minimum stresses that occur in the horizontal section of the aircraft stabilizer into a graph, they can be seen in Figure 18.

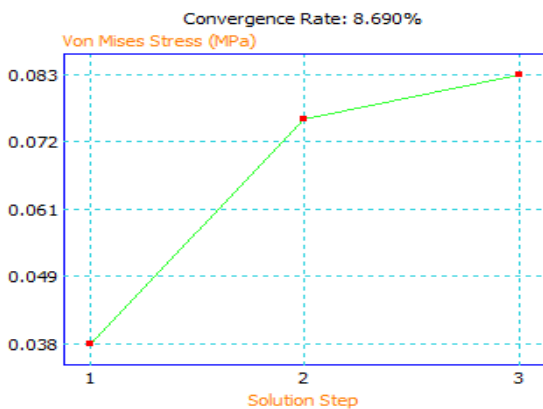


Figure 18. Stabilizer horizontal voltage graph

Figure 18 shows the minimum stress that occurs in the aircraft wing is 0.038 Mpa, the average stress distribution in the aircraft wing is 0.072 Mpa, and the maximum stress that occurs in the aircraft wing is 0.083 Mpa.

Simulation results of the stress that occurs in the vertical part of the unmanned aircraft stabilizer when it receives a load of 100N. It can be seen in Figure 19.

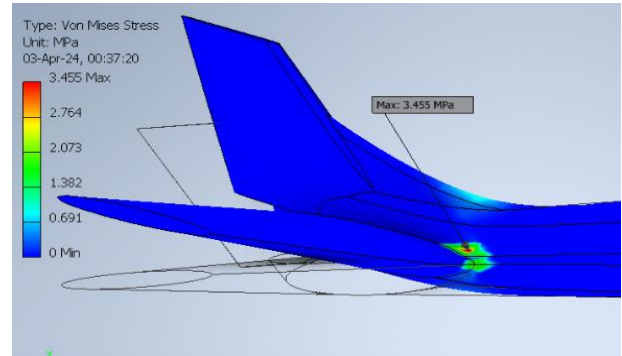


Figure 19. Vertical concentration of stabilizer.

If we describe the maximum and minimum stresses that occur in the vertical part of the aircraft stabilizer into a graph, they can be seen in Figure 20.

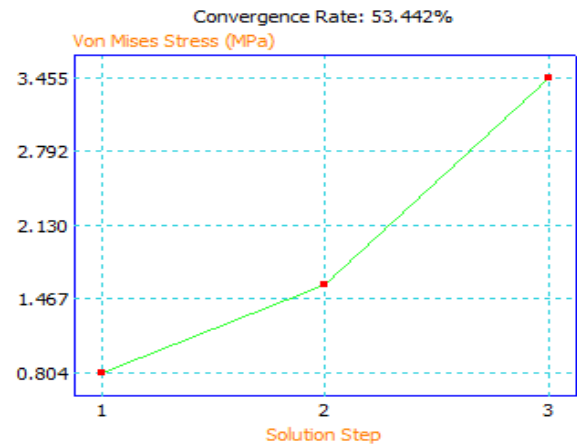


Figure 20. Stabilizer vertical stress graph

Figure 12 shows the minimum stress that occurs in the aircraft wing is 0.80 Mpa, the average stress distribution in the aircraft wing is 1.46 Mpa, and the maximum stress that occurs in the aircraft wing is 3.45 Mpa.

From the simulation results on four parts of an unmanned aircraft, including: (1) Fuselage, (2) wing, (3) horizontal stabilizer, and (4) vertical stabilizer. The voltage found that occurs throughout the entire aircraft section is presented in table 9.

Table 9. Stresses on Airplane parts.

Aircraft Components	
Fuselage	0,585 Mpa.
wing	0,429 Mpa
horizontal Stabilizer	0,083 Mpa
Vertikal Setabilizer	3,45 Mpa.

From table 9, a diagram of the distribution of stress data that occurs on the body of the unmanned aircraft that has been planned can be made. The voltage distribution diagram can be seen in Figure 21.

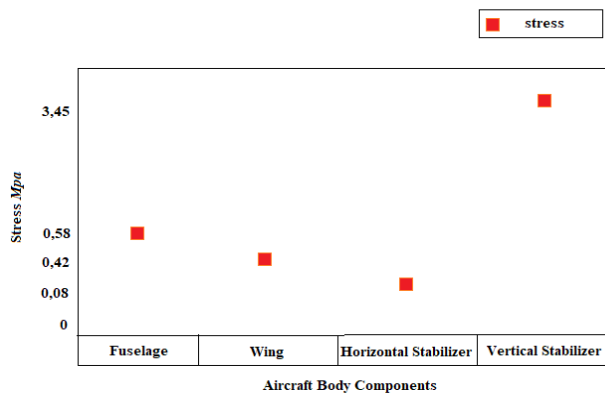


Figure 21. Stress distribution on the aircraft body.

From the stress distribution, it is clear that the stress occurs in the aircraft body. The stress that occurs in the vertical part of the stabilizer is 3.45 Mpa, the stress that occurs in the fuselage part is 0.58 Mpa, the stress that occurs in the wing part is 0.42 Mpa, and the stress that occurs in the horizontal stabilizer.

5. CONCLUSIONS

From the research, it was found that the ideal layer thickness parameter of 0.1 to 0.2 mm does not exceed half the size of the nozzle diameter of 0.4 mm to produce fine raster fibers. This is because if the layer height thickness value exceeds half the nozzle diameter, pores will appear. or gaps between layers, the impact of which will cause a decrease in the mechanical strength of the designed aircraft body frame.

From the research, it was found that the ideal speed parameter for printing a planned aircraft body frame using ABS filament material is at a speed of 30 mm/s to 50 mm/s to produce a stable raster fiber size and strong adhesion between raster fibers, if the process speed printing too fast will cause the melted ABS filament that comes out of the nozzle to cool too quickly so that the size of the raster fibers is not as stable, which causes a decrease in the adhesion between the raster fibers.

From the results of research using simulation, it can be concluded that ABS filament has great potential to be used as a material for making aircraft body frames. with a safe working load limit of 100 Newtons, the maximum stress value was found to be 3.45 MPa, while the stress value that the material could withstand from the tensile test results was 30.7 MPa at the best print parameter formula, layer height 0.15mm, gyroid infill 20% , with a speed of 30mm/s.

6. ACKNOWLEDGEMENTS

I would like to express my deepest gratitude to all the participants who took part in this study. Their willingness to share their time and experiences has been essential in providing the data needed to carry out this research.

7. AUTHOR CONTRIBUTIONS

- Conceptualization: Lazuardi Lazuardi.
- Data curation: Maryono Maryono.
- Formal analysis: Sugeng Hadi Susilo.

- Examination: Muhammad Akhlis Rizza
- Methodology: Sugeng Hadi Susilo
- Project administration: Maryono Maryono
- Source: Sugeng Hadi Susilo.
- Software: Lazuardi Lazuardi.
- Supervisor: Sugeng Hadi Susilo.
- Validation: Muhammad Akhlis Rizza.
- Visualization: Lazuardi Lazuardi, Maryono Maryono.
- Writing – original draft: Lazuardi Lazuardi
- Writing – review & editing: Muhammad Akhlis Rizza, Sugeng Hadi Susilo.

8. REFERENCES

- [1] L. Li, Q. Sun, C. Bellehumeur, and P. Gu, "Composite modeling and analysis for fabrication of FDM prototypes with locally controlled properties," *J Manuf Process*, vol. 4, no. 2, pp. 129–141, 2002, doi: 10.1016/S1526-6125(02)70139-4.
- [2] B. M. Tymrak, M. Kreiger, and J. M. Pearce, "Mechanical properties of components fabricated with open-source 3-D printers under realistic environmental conditions," *Mater Des*, vol. 58, pp. 242–246, 2014, doi: 10.1016/j.matdes.2014.02.038.
- [3] A. K. Sood, R. K. Ohdar, and S. S. Mahapatra, "Parametric appraisal of mechanical property of fused deposition modelling processed parts," *Mater Des*, vol. 31, no. 1, pp. 287–295, Jan. 2010, doi: 10.1016/j.matdes.2009.06.016.
- [4] J. Gopinathan and I. Noh, "Recent trends in bioinks for 3D printing," *Biomaterials Research*, vol. 22, no. 1. BioMed Central Ltd., Apr. 06, 2018. doi: 10.1186/s40824-018-0122-1.
- [5] O. A. Mohamed, S. H. Masood, and J. L. Bhowmik, "Optimization of fused deposition modeling process parameters: a review of current research and future prospects," *Adv Manuf*, vol. 3, no. 1, pp. 42–53, Mar. 2015, doi: 10.1007/s40436-014-0097-7.
- [6] A. Dawood, B. M. Marti, V. Sauret-Jackson, and A. Darwood, "3D printing in dentistry," *Br Dent J*, vol. 219, no. 11, pp. 521–529, Dec. 2015, doi: 10.1038/sj.bdj.2015.914.
- [7] R. B. Kristiawan, F. Imaduddin, D. Ariawan, Ubaidillah, and Z. Arifin, "A review on the fused deposition modeling (FDM) 3D printing: Filament processing, materials, and printing parameters," *Open Engineering*, vol. 11, no. 1. De Gruyter Open Ltd, pp. 639–649, Jan. 01, 2021. doi: 10.1515/eng-2021-0063.
- [8] N. Graupner, A. S. Herrmann, and J. Müssig, "Natural and man-made cellulose fibre-reinforced poly(lactic acid) (PLA) composites: An overview about mechanical characteristics and application areas," *Compos Part A Appl Sci Manuf*, vol. 40, no. 6–7, pp. 810–821, Jul. 2009, doi: 10.1016/j.compositesa.2009.04.003.
- [9] K. G. J. Christiyana, U. Chandrasekhar, and K. Venkateswarlu, "A study on the influence of

- process parameters on the Mechanical Properties of 3D printed ABS composite,” in *IOP Conference Series: Materials Science and Engineering*, Institute of Physics Publishing, Mar. 2016. doi: 10.1088/1757-899X/114/1/012109.
- [10] E. Ulu, E. Korkmaz, K. Yay, O. Burak Ozdoganlar, and L. Burak Kara, “Enhancing the Structural Performance of Additively Manufactured Objects Through Build Orientation Optimization,” *Journal of Mechanical Design*, vol. 137, no. 11, Nov. 2015, doi: 10.1115/1.4030998.
- [11] P. Ferretti *et al.*, “Relationship between fdm 3d printing parameters study: Parameter optimization for lower defects,” *Polymers (Basel)*, vol. 13, no. 13, Jul. 2021, doi: 10.3390/polym13132190.
- [12] S. Guessasma, S. Belhabib, and H. Nouri, “Effect of printing temperature on microstructure, thermal behavior and tensile properties of 3D printed nylon using fused deposition modeling,” *J Appl Polym Sci*, vol. 138, no. 14, Apr. 2021, doi: 10.1002/app.50162.
- [13] T. Letcher and M. Waytashek, “Material property testing of 3D-printed specimen in pla on an entry-level 3D printer,” in *ASME International Mechanical Engineering Congress and Exposition, Proceedings (IMECE)*, American Society of Mechanical Engineers (ASME), 2014. doi: 10.1115/IMECE2014-39379.
- [14] I. Gibson, D. W. Rosen, and B. Stucker, *Additive manufacturing technologies: Rapid prototyping to direct digital manufacturing*. Springer US, 2010. doi: 10.1007/978-1-4419-1120-9.
- [15] F. Chuanxing, W. Qi, L. Hui, Z. Quancheng, and M. Wang, “Effects of Pea Protein on the Properties of Potato Starch-Based 3D Printing Materials,” *International Journal of Food Engineering*, vol. 14, no. 3, 2018, doi: 10.1515/ijfe-2017-0297.
- [16] I. D. Savu, S. V. Savu, D. Simion, N.-A. Sîrbu, M. Ciornei, and A. Ratiu, “PP in 3D Printing- Technical and Economic Aspects.” [Online]. Available: <http://www.revmaterialeplastice.ro>
- [17] O. S. Es-Said, J. Foyos, R. Noorani, M. Mendelson, R. Marloth, and B. A. Pregger, “Effect of layer orientation on mechanical properties of rapid prototyped samples,” *Materials and Manufacturing Processes*, vol. 15, no. 1, pp. 107–122, 2000, doi: 10.1080/10426910008912976.
- [18] V. Vega *et al.*, “The effect of layer orientation on the mechanical properties and microstructure of a polymer,” *J Mater Eng Perform*, vol. 20, no. 6, pp. 978–988, Aug. 2011, doi: 10.1007/s11665-010-9740-z.
- [19] B. Pérez, H. Nykvist, A. F. Brøgger, M. B. Larsen, and M. F. Falkeborg, “Impact of macronutrients printability and 3D-printer parameters on 3D-food printing: A review,” *Food Chem*, vol. 287, pp. 249–257, Jul. 2019, doi: 10.1016/j.foodchem.2019.02.090.
- [20] E. G. Gordeev, A. S. Galushko, and V. P. Ananikov, “Improvement of quality of 3D printed objects by elimination of microscopic structural defects in fused deposition modeling,” *PLoS One*, vol. 13, no. 6, Jun. 2018, doi: 10.1371/journal.pone.0198370.